ARTICLE NO. 78-988

Effects of Propellant Temperature Gradients on Thrust Imbalance of the Space Shuttle

Richard H. Sforzini* and Winfred A. Foster Jr.†
Auburn University, Auburn, Ala.

and

Benjamin W. Shackelford Jr.‡
NASA Marshall Space Flight Center, Huntsville, Ala.

The internal ballistic effects of combined radial and circumferential grain temperature gradients are evaluated theoretically for the Space Shuttle solid rocket motors (SRM's). A simplified approach is devised for representing with closed-form mathematical expressions the temperature distribution resulting from the anticipated thermal history prior to launch. The internal ballistic effects of the gradients are established by use of a mathematical model which permits the propellant burning rate to vary circumferentially. Comparative results are presented for uniform and axisymmetric temperature distributions and the anticipated gradients based on an earlier two-dimensional analysis of the center SRM segment. The thrust imbalance potential of the booster stage is assessed based on the difference in the thermal loading of the individual SRM's of the motor pair which may be encountered in both summer and winter environments at the launch site. Results indicate that grain temperature gradients could cause the thrust imbalance to be approximately 10% higher in the Space Shuttle than the imbalance caused by SRM manufacturing and propellant physical property variability alone.

Introduction

THE large size of the solid rocket motors (SRM's) to be used in the booster stage of the Space Shuttle necessitates special attention to the effects of the temperature gradients which develop in the propellant prior to launch. The objective of this research is to investigate the effects of the temperature gradients upon the internal ballistics of the SRM's including an assessment of the potential thrust imbalance in the booster stage where two SRM's fire in parallel.

Previous analyses of the effects of thermal gradients have been confined mainly to temperatures which vary only with the distance burned (axisymmetic temperature distribution for the circular-perforated grain). While such analyses have practical application for small rocket motors, the environment to which the Space Shuttle is exposed at the launch site is such that propellant temperatures and, hence, gradients can vary significiantly in at least the radial and tangential (to the burning surface) directions.[1,2] Unlike smaller motors, it is not practical to minimize the tangential gradients by rotating the motor or by use of external insulation. Also, the thermal loading differs between the SRM's of the booster pair so that consideration must be given to the problem of the resultant thrust imbalance.

Phillips[3] presented a rigorous graphical technique for considering nonuniform burning around the burning perimeter of any cross-section of the grain. However, the method is too cumbersome to couple to a complete ballistic evaluation computer program. The approach used in this paper is that of finding a simple mathematical function which approximates the tangential temperature distribution produced by the anticipated thermal loadings on the SRM's prior to launch. The loadings are deduced in the two-dimensional thermal analysis of Refs. 1 and 2 for the summer and winter environments, respectively. The computer program described in Ref. 4, which has the rather unique capability of representing the burning geometry of out-of-round and misaligned port surfaces, is readily modified to permit analysis of the internal ballistics with the radially and tangentially varying temperatures.

Received July 14, 1978; presented as Paper 78-988 at the AIAA/SAE 14th Joint Propulsion Conference, Las Vegas, Nev., July 25-27, 1978; revision received Oct. 24, 1978.

Index categories: LV/M Propulsion and Propellant Systems; Solid and Hybrid Rocket Engines.

*Professor, Aerospace Engineering. Associate Fellow AIAA.
†Assistant Professor, Aerospace Engineering. Member AIAA.
‡Solid Propulsion Engineer, Propulsion Division.

Representation of Temperature Distributions

The propellant in the Space Shuttle consists of two identical center segments that are double tapered circularly perforated (cp) grains, an aft cp segment with a triple taper, and a forward segment with an 11-point star transitioning at roughly the midpoint of its length into a cp section. All exposed end faces are inhibited over the major portion of the slots formed when the segments are joined.

As a first approach to determining the ballistic effects of temperature gradients in the solid propellant, axial temperature gradients are neglected. Also, the analysis is focused on the cp grain sections which constitute 90% of the propellant in the Space Shuttle. Two-dimensional thermal analyses of the Space Shuttle center segments then form the basis for evaluation of the ballistic effects of grain temperature gradients. Figures 1 and 2 illustrate selected grain temperature distributions resulting from such analyses which are described in Refs. 1 and 2 for projected summer and winter environments, respectively. References 1 and 2 are comprehensive thermal evaluations based upon environments anticipated from fabrication through prelaunch at the Eastern Test Range (ETR) including separate evaluation for the east- and west-facing SRM's while on the launch pad for periods up to two months. Figures 1 and 2 illustrate the sensitivity of propellant temperature distributions to varying radiation patterns as influenced here by shading by the launch stand and the Space Shuttle orbiter and external tank.

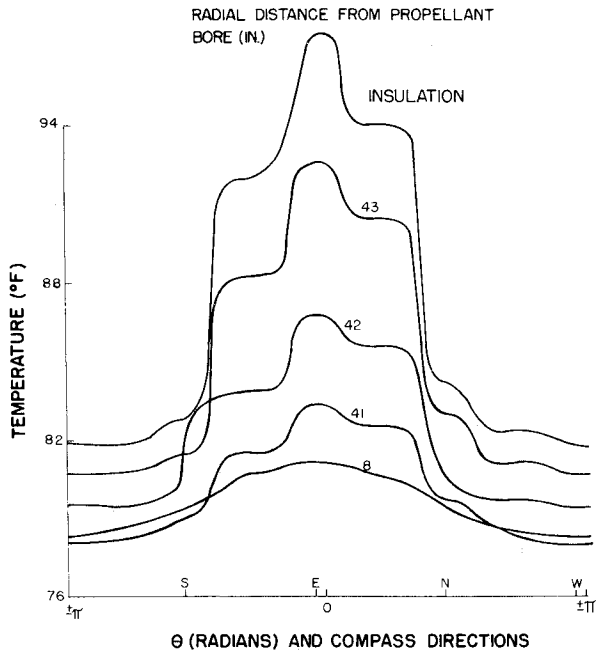

Fig. 1 Selected summer grain temperature distributions for east-facing Space Shuttle SRM.

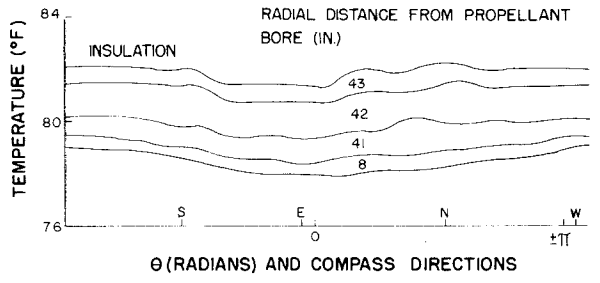

Fig. 2 Selected summer grain temperature distributions for west-facing Space Shuttle SRM.

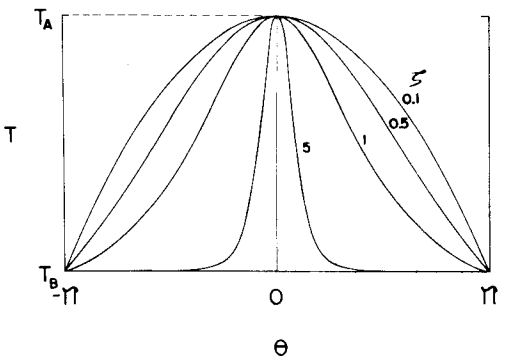

Fig. 3 Sech representation of circumferential grain temperature *(T)* distribution.

The temperature distributions shown on Figs. 1 and 2 were selected from a wide range of distributions corresponding to various periods on the launch pad and various times of the day. These particular distributions were chosen because they represent a "worst-case" situation from the standpoint of potential thrust imbalance between the east- and west-facing SRM's. Nevertheless, the forms of the given distributions are typical of those projected for the entire range of thermal loadings anticipated, including those for the winter environment. The approximate circumferential symmetry of each distribution about the radial line through the position of maximum grain temperature gradient (here, also the line of peak or minimum temperature) is especially notable. This line is designated by $\theta=0$ on Figs. 1 and 2 and in subsequent discussion.

The distributions obtained from the thermal analysis suggest a hyperbolic secant representation (Fig. 3) for the grain temperature of the form

$$T=A+B\cdot\operatorname{sech}\theta\zeta \qquad (-\pi\leq\theta\leq\pi) \tag{1}$$

where θ is the circumferential coordinate. For a given average distance burned normal to the surface, A and B are determined by the conditions

$$T=T_A \text{ at } \theta=0 \text{ and } T=T_B \text{ at } \theta=\pi \tag{2}$$

which, with Eq. (1), yield

$$T=T_A-(T_A-T_B)\,(1-\operatorname{sech}\zeta\theta)/(1-\operatorname{sech}\zeta\pi) \tag{3}$$

The subscripts A and B correspond, for one average (over the burning perimeter) distance burned, to the temperature on the radial line of maximum temperature gradients and the diametrically opposite line, respectively.

The ζ in Eq. (3) is determined from the expression

$$\zeta=c(T_A-T_{Av})/(T_{Av}-T_B) \tag{4}$$

where T_{Av} is the bulk or average temperature over the entire propellant cross-section and c is a constant determined by comparison of the hyperbolic secant representation with the results of the two-dimensional thermal analysis. The rationale of Eq. (4) is that the more concentrated the radiant heat flux near the line of maximum temperatures, the more T_A differs from T_{Av}, and the more peaked is the distribution which is reflected in a high value of ζ (see Fig. 3). Similarly, the closer T_B is to T_{Av}, the more peaked the distribution should and does become.

A trial-and-error process was used to determine c for the Space Shuttle based on the SRM with the maximum summer gradient. Values of c were calculated which cause the area under the circumferential temperature profiles calculated by Eq. (4) to match within 0.1% the areas under the corresponding profiles of Refs. 1 and 2. The c for the outermost radial position was used to recalculate profiles at 12 other radial positions. These results were compared with the corresponding profiles from Refs. 1 and 2. This process was repeated for the next two adjacent radial positions. Use of the c obtained from the outer radial position results in less accurate profile simulation toward the SRM centerline where the profiles were relatively flat. The c values for the two more inboard positions poorly model the outer profile. The significant differences between the two summer temperature distributions in the SRM pair are in the outer 3 in. and the circumferential temperature profile has the greatest range in the outer position. Therefore, the best simulation is required in that region. Because of these considerations, the outer c is chosen to model the entire temperature profile in the SRM with the maximum gradient. The final representation is compared to the two-dimensional thermal analyses results in Fig. 4. As indicated in Fig. 4, the temperature profile in the other (west-facing) SRM in that pair is flat enough to be represented adequately by the same c. The results logically lead as a matter of convenience to the use of the same c (0.075) for the SRM pair subjected to other environments. Figure 5 shows, for example, that this same value of c gives reasonable results for both SRM's in the winter "worst case" environment. Better results could, of course, be obtained by selecting separate values of c for each environment. Alternatively, the generality of the approach could be maintained while making improvements by modifying the form of Eq. (4). The results given here show that the sech representations should in general be more peaked. This could be accomplished

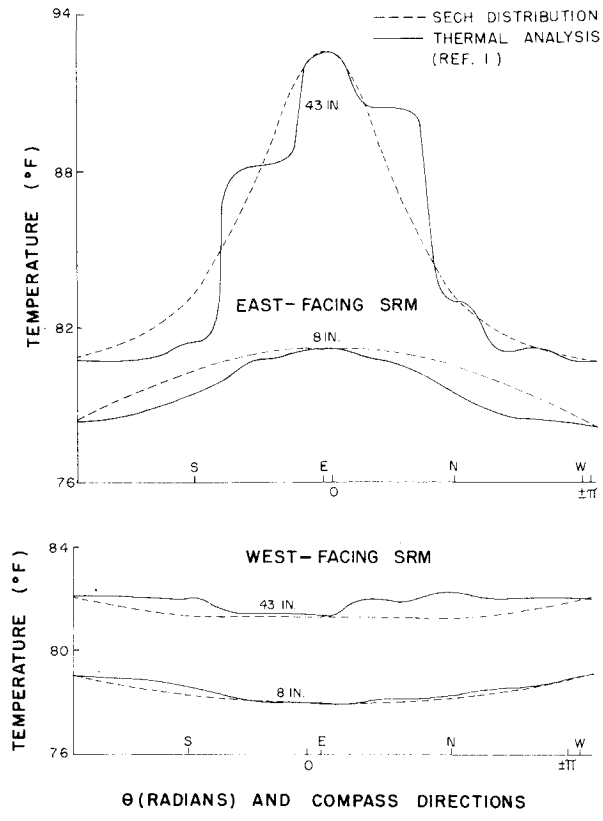

Fig. 4 Comparison of thermal analysis results with sech-distributed grain temperatures for summer worst-case.

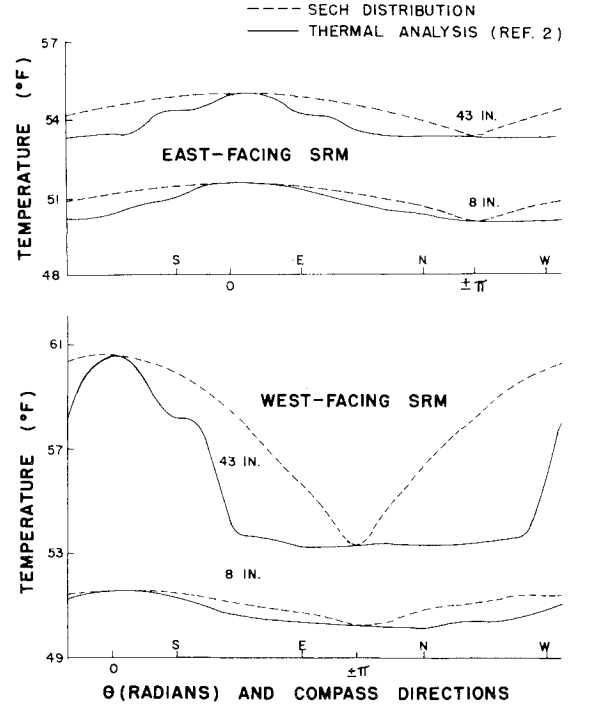

Fig. 5 Comparison of thermal analysis results with sech-distributed grain temperatures for winter worst-case.

by raising the temperature ratio in Eq. (4) to some positive power greater than 1 and redetermining c.

Internal Ballistics

The internal ballistic program described in Ref. 4 was modified as follows to accommodate the nonuniform temperature gradients defined by Eqs. (3) and (4). The only special inputs to the program required are the bulk temperature of the grain and the temperature distributions T_A and T_B along the radial line of maximum temperature gradients and the diametrically opposite line, respectively. The temperature distributions were input as tables of values at 15 radial stations. Linear interpolation was used for intermediate stations. Because of the nonuniform temperatures, the surface does not regress uniformly around the burning perimeter. The variations are accounted for in the revised program so that the temperature distributions and the resulting burning rate distributions are in effect based on the true theoretical position of the burning surface. This is accomplished by computing separate distances burned, y_A and y_B, along the two diametrically opposite radial reference lines from which the corrresponding T_A and T_B are determined. This shows, however, that an additional approximation has been made in the representation away from the reference lines because the value of c in Eq. (4) was based upon comparison of the hyperbolic secant distribution with the results of the thermal analysis at a uniform radial position.

The burning rate coefficient $\bar{a}$ is given analogous treatment to that of grain temperature. For the usual small values of burning rate sensitivity to grain temperature and practical temperature gradients, if the temperature has a hyperbolic secant distribution, $\bar{a}$ will also have a hyperbolic secant distribution to first-order accuracy. The burning rate coefficient may thus be expressed in the same form as Eq. (3) for which the average value at a given pressure in terms of burning rate coefficients is

$$\bar{a}=a_A-(a_A-a_B)\frac{1+\frac{1}{2}\zeta-(2/\pi\zeta)\arctan e^{\zeta\pi}}{1-\operatorname{sech}\zeta\pi} \tag{5}$$

Equation (5) is used to compute the mass flow rate generated by the burning surface.

In addition to affecting the mass of propellant gases generated, the temperature differences throughout the propellant influence the time first burnthrough of the propellant occurs and the characteristics of the ensuing tailoff. These effects are evaluated by coupling the present analysis with that of the ovality analysis presented in Ref. 4. In doing this, the basic features of the original analysis are retained. 1) Burning perimeters are calculated at three reference planes—one near the head of the grain, one at the aft end of the main tapered length and one at the aft end of the aft tapered length. 2) After first burnthrough, burning perimeters at the reference planes are obtained by integration:

$$S\simeq\int_{-\pi}^{\pi} r_g\,\mathrm{d}\theta \qquad r_g=0 \quad \text{if} \quad r_g\geq r_c \tag{6}$$

where r_g and θ are the polar coordinates of the burning perimeter and r_c is the radius of the grain exterior. 3) The perimeters at the reference planes are used to establish geometric correction factors which account for the effects of the nonsymmetric burning on the total burning surface area.

For use in Eq. (6), r_g is evaluated from a hyperbolic secant distributed distance burned (y) of the same form as Eq. (3). Although the distribution of distance burned is not a true hyperbolic secant distribution, our experience indicates that a good approximation is obtained in this manner when ζ is evaluated from

$$\zeta=c(y_A-\bar{y})/(\bar{y}-y_B) \tag{7}$$

where y is the average (over the burning perimeter) theoretical distance burned. It is notable that the key tailoff charac-

teristic, the time at which first grain burnthrough occurs, is not affected by the assumed y distribution since y_A is determined directly from the thermal analysis data. Use of the ovality analysis[4] permits direct coupling of the effect of grain temperature with the effect of grain out-of-roundness and/or eccentricity arising from manufacturing variations. Both effects produce thrust imbalance in the Space Shuttle SRM pair which is discussed later in this paper.

For the purpose of computing the radial temperature distribution only a cp grain was analyzed. This obviously induces some error since the results were taken as being true at corresponding distances burned in a star segment if such is also present. However, heating or cooling is primarily from the outside of the motor case and propellant is an efficient insulator, so at least the inner portion of the propellant, including the star points, should be at nearly the same temperature in the star and cp grain segments. Also, the star grain burns out much earlier than the cp grain, which tends to minimize the effect of the star grain temperature distribution on the critical tailoff phase of operation.

To obtain an indication of the extent of error associated with the commonly used simplifying assumptions of uniform or axisymmetric temperature gradients, the thrust vs time characteristics of the Space Shuttle were evaluated for three different temperature distribution cases: 1) a hyperbolic secant distibution based on the results of the thermal analysis of the east-facing SRM for the worst-case summer environment at the ETR (Fig. 1), 2) a uniform temperature distribution at the bulk temperature of case 1, and 3) an axisymmetric distribution defined by the profile along the radial reference line of maximum temperature gradients for case 1. The results are given in Fig. 6 in terms of the thrust imbalance (difference) vs time between cases 1 and 2 and cases 1 and 3. For the purpose of discussion, it is assumed that the hyperbolic secant distribution represents the real distribution of temperatures within the grain. Then, as Fig. 6 indicates, a maximum error of approximately 19,000 lb_f is made in the thrust calculation by assuming the uniform grain temperature. On the other hand, if the axisymmetric temperature distribtuion is assumed, the maximum error is approximately 45,000 lb_f. A separate calculation yields a maximum thrust difference of approximately 64,000 lb_f between cases 2 and 3 as might be anticipated from the other two comparisons. This shows that the assumption of an axisymmetric gradient for the Space Shuttle SRM would yield at best an ultraconservative estimate of the effects of nonuniformity of grain temperature on the performance of a single SRM.

Thrust Imbalance

Although 19,000-lb_f thrust differential represents less than 1% of the nominal thrust level of a Space Shuttle SRM, when the separate temperature distributions in a pair of SRM's used in a singler booster stage are considered, additional thrust imbalance can arise. Figures 7 and 8 give the resultant thrust imbalance calculated using sech temperature distributions for both SRM's for the worst-case summer and winter launches, respectively. The corresponding maximum thrust imbalances are approximately 83,000 and 46,000 lb_f, respectively. These imbalances represent small but significant fractions of the stage thrust and should be considered in analysis of performance along with the other sources of thrust imbalance which establish control system requirements. In Ref. 4, the Space Shuttle thrust imbalance was analyzed theoretically without regard to temperature distribution effects. The statistical evaluation yielded a predicted limit of thrust imbalance of $\pm 580{,}200$ lb_f (90% probability for 99.9% of the total population). For the present paper, the imbalance limits are reassessed at $\pm 405{,}500$ lb_f, still without consideration of temperature gradients. The lower number results from design changes made in the original configuration for the purpose of reducing thrust imbalance and from refinements in the details of the anlysis procedure.

The latter limits must now be extended to account for the temperature distribution effects. Although the gradients used in obtaining Fig. 7 have been termed the worst-case, this has no firm statistical basis. It is now suggested with some arbitrariness, but with the idea of obtaining a degree of conservatism, that the summer worst-case results represents two standard deviations in the thrust imbalance due to temperature distribution effects. Then the total thrust imbalance limits predicted are $\pm 448{,}200$. This is based on the root-mean-square law applied to the standard deviation in thrust imbalance due to temperature distribution differences and that due to all other effects (88,160 lb_f). A two-sided confidence coefficient of 3.833 based on the sample size of 50 SRM pairs is used as it was in Ref. 4 for assessing the thrust

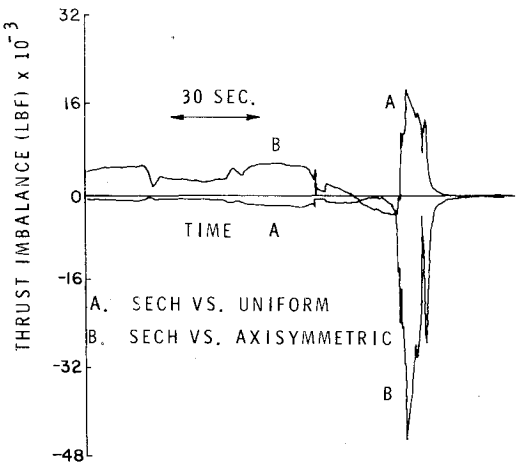

Fig. 6 Thrust imbalance due to different assumed grain temperature distributions for Space Shuttle SRM pair.

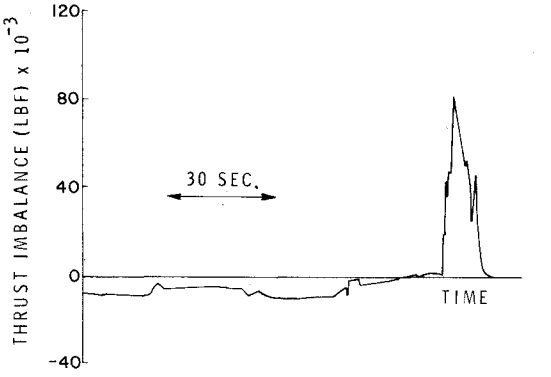

Fig. 7 SRM pair thrust imbalance due to temperature differences for summer launch (sech temperature distribution).

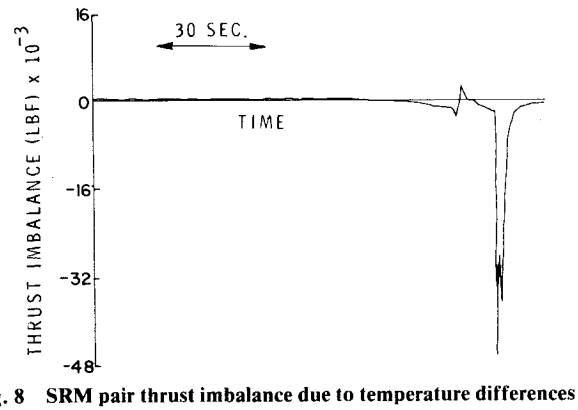

Fig. 8 SRM pair thrust imbalance due to temperature differences for winter launch (sech temperature distribution).

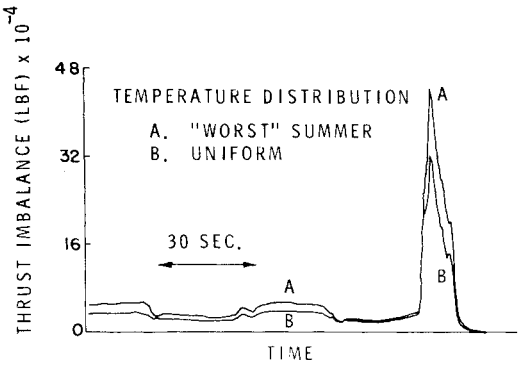

Fig. 9 Monte Carlo evaluation of range of thrust imbalance for summer launch.

imbalance without regard to temperature distribution differences.

The thrust imbalance limits given include a multiplying factor of 1.2 to account for differences between theoretical and experimental results based on analyses of Titan IIIC SRM's.[4] It is possible that temperature distribution differences in the Titan IIIC SRM pairs may have contributed to this factor. However, insufficient quantitative data are available to establish the temperature differences, and qualitative information indicates that the temperature differences were less pronounced for the Titan pairs than those anticipated for the Space Shuttle. In any event, retention of the 1.2 factor adds further conservatism to the evaluation.

The validity of the method of combining the thrust imbalance was tested by a final reassessment of thrust imbalance using the worst-case summer gradients with a Monte Carlo reassessment[4] of the thrust imbalance due to other causes. For this check, the imbalance due to temperature distribution differences is taken as one standard deviation to be consistent with the use of the same two nonuniform temperature distributions for each pair of SRM's in the Monte Carlo evaluation. Practically identical results were obtained for the maximum thrust imbalance to those obtained by the root-mean-square law, indicating that the temperature gradient effects are not coupled to those of the other sources of thrust imbalance. The resultant imbalance range vs time is shown on Fig. 9 along with the results for an assessment without temperature gradients. The 1.2 factor is not incorporated in Fig. 9 because it is strictly applicable only to the maximum thrust imbalance calculated without regard to where it occurs, whereas Fig. 9 is based on statistical analysis of the thrust imbalance at specific times. Analyses of the Titan IIIC using the Monte Carlo method yielded maximum thrust imbalance values that were approximately 4% higher than test data when the imbalance limits were calculated at specific times.[5]

Concluding Remarks

The relatively simple scheme for representation of the gradients presented here can, of course, be no better than the thermal analysis which it simulates and is limited to two-dimensional representations of cp grains. Nevertheless, it makes assessment of the effects of realistic grain temperature distributions practical. The approach clearly establishes the magnitude of error associated with the common assumptions of uniform or axisymmetric gradients.

Results of the theoretical analysis of thrust imbalance for the Space Shuttle show that the imbalance limits for launch at the ETR are increased by about 10% due to grain temperature gradients. It has also been established that the effect may be computed separately and combined statistically with thrust imbalance from other sources using the root-mean-squares of the respective standard deviations.

Acknowledgments

This research was performed at George C. Marshall Space Flight Center (MSFC), National Aeronautics and Space Administration (NASA) and at Auburn University under Modifications Nos. 14 and 19 to the Cooperative Agreement, dated Feb. 11, 1969, between MSFC and Auburn University, NCA8-00106 and NCA8-00125, respectively.

References

[1] Grenda, R. B., "A Two-Dimensional Thermal Analysis of the SRM Center Segment During Exposure to a Summer Environment at the ETR." Wasatch Div., Thiokol Corporation, Doc. No. TWR-10822, Dec. 24, 1975.

[2] Grenda, R. B., "A Two-Dimensional Thermal Analysis of the SRM Center Segment During Exposure to a Winter Environment at ETR," Wasatch Div., Thiokol Corporation, Doc. No. TWR-11104, July 12, 1975.

[3] Phillips, B. R. and Tanger, G. E., "Effects of Nonuniform Grain Temperature on Solid Propellant Motor Ballistic Parameters," *ARS Journal*, Vol. 32, June 1962, p. 969.

[4] Sforzini, R. H. and Foster, W. A., Jr., "Monte Carlo Investigation of Thrust Imbalance of Solid Rocket Motor Pairs," *Journal of Spacecraft and Rockets*, Vol. 13, April 1976, pp. 198-202.

[5] Sforzini, R. H. and Foster, W. A., Jr., "Solid-Propellant Rocket Motor Ballistic Performance Variation Analyses (Phase Two)," Auburn University, NASA CR-150324, Sept. 1976, p. 11.